Steel and Composite Structures, *Vol. 34, No. 5 (2020) 657-670*
DOI: https://doi.org/10.12989/scs.2020.34.5.657

Three dimensional free vibration analysis of functionally graded nano cylindrical shell considering thickness stretching effect

Maryam Lori Dehsaraji, Mohammad Arefi* and Abbas Loghman

Department of Solid Mechanics, Faculty of Mechanical Engineering, University of Kashan, Kashan, Iran

(*Received April 17, 2019, Revised January 10, 2020, Accepted January 27, 2020*)

Abstract. In this paper, vibration analysis of functionally graded nanoshell is studied based on the sinusoidal higher-order shear and normal deformation theory to account thickness stretching effect. To account size-dependency, Eringen nonlocal elasticity theory is used. For more accurate modeling the problem and corresponding numerical results, sinusoidal higher-order shear and normal deformation theory including out of plane normal strain is employed in this paper. The radial displacement is decomposed into three terms to show variation along the thickness direction. Governing differential equations of motion are derived using Hamilton's principle. It is assumed that the cylindrical shell is made of an arbitrary composition of metal and ceramic in which the local material properties are measured based on power law distribution. To justify trueness and necessity of this work, a comprehensive comparison with some lower order and lower dimension works and also some 3D works is presented. After presentation of comparative study, full numerical results are presented in terms of significant parameters of the problem such as small scale parameter, length to radius ratio, thickness to radius ratio, and number of modes.

Keywords: thickness stretching effect; shear and normal deformation theory; free vibration analysis; length scale parameter; nonlocal theory

1. Introduction

According to extended application of materials and structures in very small scales (micro or nano) in recent years, some researchers investigated on the various aspects of nanomaterials (Yildirm 1999, Chen *et al.* 2008, Gholami *et al.* 2016, Baghani *et al.* 2016, Zhu *et al.* 2017). The response of structures in very small scales basically differs from that in macro scales. For modeling the structures in small scales, the continuum theory does not lead to acceptable results. It was concluded that the modeling of the structures in small scales needs to be corrected by accounting some small scale parameters. Some theories considering the size effects such as Eringen nonlocal elasticity theory (Eringen 1983), modified couple stress theory (MCST) by Gurtin and Murdoch (1975), strain gradient theory (SGT) Gurtin and Murdoch (1978) and the surface stress theory (SST) (Yang *et al.* 2002, Gurtin *et al.* 1998, Lam *et al.* 2003) have been developed by various researchers. Some important works on the dynamic behaviors of nano sized structures have been presented (Moradi-Dastjerdi *et al.* 2014, Tadi Beni 2016, Shojaeefard *et al.* 2018).

The application of nonlocal theory on vibration analysis of nanobeams, nanoshells and carbon nanotubes (CNTs) has been presented by some researchers (Wang 2005, Ansari *et al.* 2012). Ansari *et al.* (2011) used a nonlocal shell model for the vibration analysis of double-walled CNTs with different boundary conditions. They indicated that, with considering appropriate values of nonlocal parameter to predict the free vibration behavior, good results are obtained that are comparable with the results of molecular dynamics simulations. She *et al*. (2017) used the nonlocal theory for analysis of the thermal buckling and postbuckling behavior of porous tubes. They showed that the critical temperature and post-buckling strength of the tube increases with the increase of porosity volume fraction.

The Eringen's nonlocal theory is included one small scale parameter. Some researchers such as Koutsoumaris *et al.* (2017), Shaat and Abdelkefi (2017) showed that one scaling parameter is insufficient to predict mechanical behavior of nanostructures. Thus, other theories were presented that including two scale parameters. Safaei *et al*. (2018) investigated dynamic behavior of nanocomposite sandwich plates under periodic thermo-mechanical loadings. Vibration and buckling analysis of piezoelectric nanoplate with considering the surface effects based on the modified Kirchhoff plate model was studied by Yan *et al.* 2012 to investigate critical electric voltage of buckling. Wang *et al*. (2013) studied large amplitude free vibration of circular micro-plates based on the modified couple stress theory (MCST). They indicated that increase of small scale parameter leads to significant increase of the frequency of the plate, however does not significant effect on the fundamental mode shape. Salehipour (2015) used MCST and three-dimensional elasticity theory for exact free vibration analysis of functionally graded nano/micro-plates. It was concluded that increase of length scale parameter leads to increase of the rigidity and the natural frequencies

*Corresponding author, Associate Professor
E-mail: arefi@kashanu.ac.ir; arefi63@gmail.com

ISSN: 1229-9367 (Print), 1598-6233 (Online)

especially for out-of-plane modes compared with the frequencies of the in-plane modes.

Dynamic behavior of single-walled carbon nanotubes using the nonlocal theory and the three dimensional elasticity theory has been studied by Alibeigloo *et al.* 2013. Zeighampour *et al.* (2014) studied the dynamic behavior of double walled conveying fluid carbon nanotube using modified couple stress theory. They studied on the effect of small scale parameter and fluid velocity parameters on the results obtained from the classical theory and MCST. Murmu *et al.* (2011) analyzed torsional vibration of single-walled carbon nanotubes using nonlocal beam theory. Ansari *et al.* (2011) used Donnell shell model for free vibration and buckling behavior of carbon nanotube based on nonlocal theory. Ghavanloo and Fazelzadeh (2013) studied shell-like vibration of carbon nanotubes with arbitrary chirality as an anisotropic elastic shell model. Pourasghar *et al.* (2016) studied the three-dimensional thermo-elastic analysis of functionally graded carbon nanotube subjected to thermal environment using generalized differential quadrature method. There are more papers which presented general studies on modeling of nanotubes based on nonlocal elasticity theory (Reddy 2007, Zhang *et al.* 2009, Arash and Wang 2012, Wang *et al*. 2015, Daneshmand *et al*. 2013). Li *et al.* (2017) studied the thermo-electro-mechanical transverse vibration and stability of viscoelastic piezoelectric nanoplate.

Arefi and Zenkour (2016) investigated effect of electric potential on free vibration, wave propagation and tension analyses of sandwich micro/nanorod based on strain gradient theory (SGT). Xiang and Yang (2016) studied the free and forced vibration of laminated functionally graded beams under thermal load using the first-order shear deformation beam theory. Pradhan and Phadikar (2009) analyzed the vibration of multi-layered graphene sheets with considering the small scale parameter based on the nonlocal classical plate theory. Hosseini *et al*. (2018) analyzed vibration of deep curved FG nanobeam based on modified couple stress theory. Tadi Beni *et al*. (2015) presented the free vibration of functionally graded cylindrical nanoshell based on the modified couple stress theory and first-order shear deformation theory. Soleimani *et al.* (2018) used a finite element model for vibration analysis of nanoshell. Analysis of the thin cylindrical shell based on modified couple stress theory and the first-order shear deformation theory was performed by Zeighampour and Tadi Beni (2015). Belkorissat *et al.* (2015) applied a new nonlocal hyperbolic refined plate model for free vibration of FG plates. Rabczuk *et al.* (2007, 2010) developed some numerical methods for modeling the fluid–structure interaction and non-linear dynamic fracture. Nguyen-Thanh (2017) studied a coupled problem for large deformation analysis of thin shells. Amiri et al (2016) and Areias *et al.* (2014) studied application of Phase-field modeling on the fracture of thin shells and plates including finite strains. Guo *et al*. (2019) studied bending analysis of Kirchhoff plate using deep collocation method. Javvaji *et al.* (2018) used highly electrically conductive graphene in solar cells for future generation of photovoltaics. The fracture properties were calculated using the molecular dynamics simulations in uniaxial tension. Budarapu *et al.* (2017a) proposed a solid shell-based adaptive atomistic–continuum numerical method for simulation of crack growth in thin-walled structures based on a hybrid solid shell formulation. Budarapu *et al.* (2017b) studied the effect of small scales on the mechanical behavior of systems. They presented some advantages of the multiscale methods to reduce the computational costs. Budarapu *et al.* (2014) proposed a coarse-graining method for continuum modeling of complex cracks. They used some useful methods to separate the atoms on the crack surface from other atoms.

A comprehensive literature review was completed above based on focus on the works related to size dependent analysis, higher-order shear deformation theory and free vibration analysis of cylindrical shells. This review indicates that there is no published work on the application of sinusoidal higher-order shear and normal deformation theory to nonlocal free vibration analysis of cylindrical nano shells accounting thickness stretching. In this paper, three dimensional free vibration analysis of functionally graded nanoshell based nonlocal theory is investigated based on the higher order shear and normal deformation theory with considering thickness stretching effects. It is assumed that material properties vary through the thickness direction according to volume fraction of metal and ceramic. The analytical solution is proposed to investigate the effect of various significant parameters such as small scale parameter, some dimensionless geometric ratios such as thickness to radius and length to radius ratios and mode number on the natural frequencies of nano shell. Before presentation of complete numerical results, a comprehensive verification using comparison with previous works is presented. In addition, for justifying the importance of the present formulation and corresponding numerical results, the numerical results are presented and compared with and without thickness stretching effect.

2. Constitutive relations based on the HOSNDT

The FG cylindrical nanoshell with length L, radius R and thickness h. FGM is usually made of a combination of two materials such as ceramic and metal. The material properties of the FG cylindrical shell varies continuously and uniformly from ceramic properties at the inner surface of the cylindrical nanoshell to the properties of the metal at the outer surface as a function of volume fraction of ceramic and metal according to power law distribution along the thickness direction as

$$V_m = \left(\frac{z}{h} + \frac{1}{2}\right)^N \qquad V_c = 1 - V_m \tag{1}$$

In which, N is inhomogeneous index. The variable material properties of the cylindrical nanoshell including modulus of elasticity and density are expressed as (Arefi and Zenkour 2017)

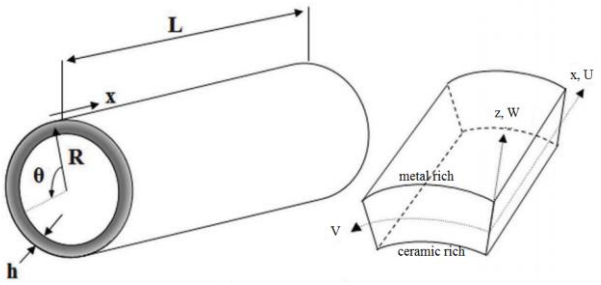

Fig. 1 The schematic figure of a FG cylindrical nanoshell

$$E(z)=(E_m-E_c)(\frac{z}{h}+\frac{1}{2})^N+E_c$$
$$\rho(z)=(\rho_m-\rho_c)(\frac{z}{h}+\frac{1}{2})^N+\rho_c \tag{2}$$

Where E_c and ρ_c are obtained at $z=-\frac{h}{2}$, E_m and ρ_m are obtained at $z=\frac{h}{2}$, which respectively represent Young's modulus and density of ceramic and metal. It should be noted that, the Poisson's ratio is assumed constant along the thickness of FG nanoshell. Based on the information of Fig. 1, the displacement field of cylindrical nanoshell based higher-order shear and normal deformation shell theory with thickness stretching effect is expressed as

$$U(x,\theta,z)=u_0(x,\theta)-z\frac{\partial w}{\partial x}(x,\theta)-\psi_1\frac{\partial \phi}{\partial x}(x,\theta)$$
$$V(x,\theta,z)=v_0(x,\theta)-\frac{z}{r}\frac{\partial w}{\partial \theta}(x,\theta)-\psi_1\frac{1}{r}\frac{\partial \phi}{\partial \theta}(x,\theta) \tag{3}$$
$$W(x,\theta,z)=w(x,\theta)+\phi(x,\theta)+\psi_2\ \chi(x,\theta)$$

In which, $u_0(x,\theta)$ and $v_0(x,\theta)$ are displacements of middle surface, $w(x,\theta)$ and $\phi(x,\theta)$ are the bending and shear components of the lateral displacement W, and $\chi(x,\theta)$ is an additional function of x and θ. It is concluded that the third term in radial displacement of Eq. (3) is employed for thickness stretching effect.

The presented two-unknown functions of shear and normal deformation theory is given with more details from Zenkour (2013)

$$\psi_1=(z-\frac{h}{\pi}\sin(\frac{\pi z}{h}))$$
$$\psi_2=\cos(\frac{\pi z}{h}) \tag{4}$$

Eq. (4) indicates that the present theory is sinusoidal shear and normal deformation theory. Based on the displacement field, the strain components are expressed as

$$\varepsilon_x=\frac{\partial U}{\partial x}=\frac{\partial u_0}{\partial x}-z\frac{\partial^2 w}{\partial x^2}-\psi_1\frac{\partial^2 \phi}{\partial x^2}$$
$$\varepsilon_\theta=\frac{1}{r}\frac{\partial V}{\partial \theta}+\frac{W}{r}=\frac{1}{R+z}\frac{\partial V_0}{\partial \theta}-\frac{z}{(R+z)^2}\frac{\partial^2 w}{\partial \theta^2}$$
$$-\frac{\psi_1}{(R+z)^2}\frac{\partial^2 \phi}{\partial \theta^2}+\frac{w}{R+z}+\frac{\phi}{R+z}+\frac{\psi_2}{R+z}\chi$$
$$\varepsilon_z=\frac{\partial W}{\partial z}=\frac{\partial \psi_2}{\partial z}\chi$$

$$\varepsilon_{z\theta}=\frac{1}{2}(\frac{1}{r}\frac{\partial W}{\partial \theta}+\frac{\partial V}{\partial z}-\frac{V}{r})=\frac{1}{2}\Big[\frac{2z}{(R+z)^2}\frac{\partial w}{\partial \theta}+ \tag{5}$$
$$(\frac{\psi_2}{R+z}+\frac{2\psi_1}{(R+z)^2})\frac{\partial \phi}{\partial \theta}+\frac{\psi_2}{R+z}\frac{\partial \chi}{\partial \theta}-\frac{1}{(R+z)}v_0\Big]$$
$$\varepsilon_{xz}=\frac{1}{2}(\frac{\partial U}{\partial z}+\frac{\partial W}{\partial x})=\frac{1}{2}\Big[\psi_2\frac{\partial \phi}{\partial x}+\psi_2\frac{\partial \chi}{\partial x}\Big]$$
$$\varepsilon_{\theta x}=\frac{1}{2}(\frac{\partial V}{\partial x}+\frac{1}{r}\frac{\partial U}{\partial \theta})=\frac{1}{2}\Big[\frac{\partial v_0}{\partial x}-\frac{2z}{R+z}\frac{\partial^2 w}{\partial \theta \partial x}$$
$$-\frac{2\psi_1}{R+z}\frac{\partial^2 \phi}{\partial \theta \partial x}+\frac{1}{R+z}\frac{\partial u_0}{\partial \theta}\Big]$$

The constitutive relation is expressed as

$$\sigma_{ij}=C_{ijkl}\,\varepsilon_{kl} \tag{6}$$

In which C_{ijkl} represents the stiffness coefficients. Based on the three-dimensional analysis, the stiffness coefficients are expressed in terms of Young's modulus and Poisson's ratio. The developed constitutive relations (Eq. (6)) in three-dimensional coordinate system are expressed as

$$\sigma_{xx}=\frac{E}{(1+\upsilon)(1-2\upsilon)}\big[(1-\upsilon)\varepsilon_{xx}+\upsilon(\varepsilon_{\theta\theta}+\varepsilon_{zz})\big]$$
$$\sigma_{\theta\theta}=\frac{E}{(1+\upsilon)(1-2\upsilon)}\big[(1-\upsilon)\varepsilon_{\theta\theta}+\upsilon(\varepsilon_{zz}+\varepsilon_{xx})\big]$$
$$\sigma_{zz}=\frac{E}{(1+\upsilon)(1-2\upsilon)}\big[(1-\upsilon)\varepsilon_{zz}+\upsilon(\varepsilon_{\theta\theta}+\varepsilon_{xx})\big]$$
$$\tau_{z\theta}=\frac{E}{(1+\upsilon)}\varepsilon_{z\theta} \tag{7}$$
$$\tau_{zx}=\frac{E}{(1+\upsilon)}\varepsilon_{zx}$$
$$\tau_{x\theta}=\frac{E}{(1+\upsilon)}\varepsilon_{x\theta}$$

To show the behavior of structures in nanoscale, the nonlocal elasticity theory is used, that was developed by Eringen (1983). The nonlocal stress–strain relations are expressed based on the Ref (Duan *et al*. 2007, Arefi and Zenkout 2017a, b, c, d, e, 2019) as

$$(1-L_1{}^2\nabla^2)\sigma_{ij}=C_{ijkl}\,\varepsilon_{kl} \tag{8}$$

In which L_1 is the nonlocal parameter, ∇^2 is the Laplacian operator that can be developed in cylindrical coordinate system as

$$\nabla^2=\frac{\partial^2}{\partial x^2}+\frac{1}{(R+z)^2}\frac{\partial^2}{\partial\theta^2} \tag{9}$$

By substitution of strain components, we obtain the stress components (Eq. (7)) as

$$\begin{aligned}
(1-L_1{}^2\nabla^2)\sigma_{zz} &= \frac{E}{(1+\upsilon)(1-2\upsilon)}\Bigg[(1-\upsilon)(\frac{\partial\psi_2}{\partial z}\,\chi)\\
&+\upsilon(\frac{\partial u_0}{\partial x}-z\,\frac{\partial^2 w}{\partial x^2}-\psi_1\frac{\partial^2\phi}{\partial x^2}+\frac{1}{R+z}\frac{\partial V_0}{\partial\theta}\\
&-\frac{z}{(R+z)^2}\frac{\partial^2 w}{\partial\theta^2}-\frac{\psi_1}{(R+z)^2}\frac{\partial^2\phi}{\partial\theta^2}+\frac{w}{R+z}\\
&+\frac{\phi}{R+z}+\frac{\psi_2}{R+z}\,\chi)\Bigg]\\
(1-L_1{}^2\nabla^2)\sigma_{\theta\theta} &= \frac{E}{(1+\upsilon)(1-2\upsilon)}\Bigg[(1-\upsilon)(\frac{1}{R+z}\frac{\partial V_0}{\partial\theta}\\
&-\frac{z}{(R+z)^2}\frac{\partial^2 w}{\partial\theta^2}-\frac{\psi_1}{(R+z)^2}\frac{\partial^2\phi}{\partial\theta^2}+\frac{w}{R+z}+\frac{\phi}{R+z}\\
&+\frac{\psi 2}{R+z}\,\chi)+\upsilon(\frac{\partial u_0}{\partial x}-z\,\frac{\partial^2 w}{\partial x^2}-\psi_1\frac{\partial^2\phi}{\partial x^2}+\frac{\partial\psi_2}{\partial z}\,\chi)\Bigg]\\
(1-L_1{}^2\nabla^2)\sigma_{xx} &= \frac{E}{(1+\upsilon)(1-2\upsilon)}\Bigg[(1-\upsilon)(\frac{\partial u_0}{\partial x}\\
&-z\,\frac{\partial^2 w}{\partial x^2}-\psi_1\frac{\partial^2\phi}{\partial x^2})+\upsilon(\frac{1}{R+z}\frac{\partial V_0}{\partial\theta}-\frac{z}{(R+z)^2}\frac{\partial^2 w}{\partial\theta^2}\\
&-\frac{\psi_1}{(R+z)^2}\frac{\partial^2\phi}{\partial\theta^2}+\frac{w}{R+z}+\frac{\phi}{R+z}+\frac{\psi_2}{R+z}+\frac{\partial\psi_2}{\partial z}\,\chi)\Bigg]\\
(1-L_1{}^2\nabla^2)\tau_{z\theta} &= \frac{E}{2(1+\upsilon)}\Bigg[\frac{2z}{(R+z)^2}\frac{\partial w}{\partial\theta}+(\frac{\psi_2}{R+z}\\
&+\frac{2\psi_1}{(R+z)^2})\frac{\partial\phi}{\partial\theta}+\frac{\psi_2}{R+z}\frac{\partial\chi}{\partial\theta}-\frac{1}{(R+z)}v_0\Bigg]\\
(1-L_1{}^2\nabla^2)\tau_{x\theta} &= \frac{E}{2(1+\upsilon)}\Bigg[\frac{\partial v_0}{\partial x}-\frac{2z}{R+z}\frac{\partial^2 w}{\partial\theta\partial x}-\\
&\frac{2\psi_1}{R+z}\frac{\partial^2\phi}{\partial\theta\partial x}+\frac{1}{R+z}\frac{\partial u_0}{\partial\theta}\Bigg]\\
(1-L_1{}^2\nabla^2)\tau_{zx} &= \frac{E}{2(1+\upsilon)}\Bigg[\psi_2\frac{\partial\phi}{\partial x}+\psi_2\frac{\partial\chi}{\partial x}\Bigg]
\end{aligned} \tag{10}$$

The governing equations of motion are derived from Hamilton's principle as follows

$$\int_{t_1}^{t_2}\delta T-\delta U+\delta W\,dt=0 \tag{11}$$

In which U, T and W are strain energy, kinetic energy, and energy of external works, respectively. Variation of strain energy is expressed as

$$\begin{aligned}
\delta U=\iiint\{&\sigma_z\delta\varepsilon_z+\sigma_\theta\delta\varepsilon_\theta+\sigma_x\delta\varepsilon_x+\tau_{z\theta}\delta\gamma_{z\theta}\\
&+\tau_{zx}\delta\gamma_{zx}+\tau_{x\theta}\delta\gamma_{x\theta}\}(R+z)dzd\theta dx
\end{aligned} \tag{12}$$

Substitution of strain components into Eq. (12) and integration leads to following relations

$$\begin{aligned}
\delta U=&\,\delta u_0\{-(R+z)\frac{\partial\sigma_x}{\partial x}-\frac{\partial\tau_{x\theta}}{\partial\theta}\}+\\
&\delta v_0\{-\frac{\partial\sigma_\theta}{\partial\theta}-(R+z)\frac{\partial\tau_{x\theta}}{\partial x}-\tau_{\theta z}\}+\\
&\delta\chi\{(R+z)\frac{\partial\psi_2}{\partial z}\sigma_z+\psi_2\sigma_\theta-\psi_2\frac{\partial\tau_{\theta z}}{\partial\theta}-\\
&(R+z)\psi_2\frac{\partial\tau_{xz}}{\partial x}\}+\delta w\{-\frac{z}{R+z}\frac{\partial^2\sigma_\theta}{\partial\theta^2}+\\
&\sigma_\theta-z(R+z)\frac{\partial^2\sigma_x}{\partial x^2}-2z\frac{\partial^2\tau_{x\theta}}{\partial x\partial\theta}-\\
&\frac{2z}{(R+z)}\frac{\partial\tau_{\theta z}}{\partial\theta}\}+\delta\phi\{-\frac{\psi_1}{(R+z)}\frac{\partial^2\sigma_\theta}{\partial\theta^2}+\sigma_\theta-\\
&\psi_1(R+z)\frac{\partial^2\sigma_x}{\partial x^2}-2\psi_1\frac{\partial^2\tau_{x\theta}}{\partial x\partial\theta}\\
&-(\psi_2+\frac{2\psi_1}{(R+z)})\frac{\partial\tau_{\theta z}}{\partial\theta}-\psi_2(R+z)\frac{\partial\tau_{xz}}{\partial x}\}
\end{aligned} \tag{13}$$

Substitution of stress components into Eq. (13), yields variation of strain energy in terms of resultant components as follows

$$\begin{aligned}
\delta U=&\,\delta u_0\Big[-R\frac{\partial N^0_{xx}}{\partial x}-\frac{\partial M^0_{xx}}{\partial x}-\frac{\partial N^0_{x\theta}}{\partial\theta}\Big]+\\
&\delta v_0\Big[-\frac{\partial N^0_{\theta\theta}}{\partial\theta}-R\frac{\partial N^0_{x\theta}}{\partial x}-\frac{\partial M^0_{x\theta}}{\partial x}-N^0_{\theta z}\Big]+\\
&\delta\chi[R\,D^{00}_{zz}+D^{01}_{zz}+B^{00}_{\theta\theta}-\frac{\partial B^{00}_{\theta z}}{\partial\theta}-R\frac{\partial B^{00}_{xz}}{\partial x}\\
&-\frac{\partial B^{01}_{xz}}{\partial x}]+\delta w[-\frac{\partial^2 M^1_{\theta\theta}}{\partial\theta^2}+N^0_{\theta\theta}-R\frac{\partial^2 M^0_{xx}}{\partial x^2}-\\
&\frac{\partial^2 E^0_{xx}}{\partial x^2}-2\frac{\partial^2 M^0_{x\theta}}{\partial x\partial\theta}-\frac{\partial N^0_{\theta z}}{\partial\theta}+R\frac{\partial N^1_{\theta z}}{\partial\theta}-\frac{\partial M^1_{\theta z}}{\partial\theta}]+\\
&\delta\phi[-\frac{\partial^2 A^{10}_{\theta\theta}}{\partial\theta^2}+N^0_{\theta\theta}-R\frac{\partial^2 A^{00}_{xx}}{\partial x^2}-\frac{\partial^2 A^{01}_{xx}}{\partial x^2}-\\
&2\frac{\partial^2 A^{00}_{x\theta}}{\partial x\partial\theta}-\frac{\partial N^0_{\theta z}}{\partial\theta}+\frac{\partial C^{00}_{\theta z}}{\partial\theta}-2\frac{\partial A^{01}_{\theta z}}{\partial\theta}+R\frac{\partial C^{00}_{xz}}{\partial x}+\\
&\frac{\partial C^{01}_{xz}}{\partial x}-R\frac{\partial N^0_{xz}}{\partial x}-\frac{\partial M^0_{xz}}{\partial x}]
\end{aligned} \tag{14}$$

The variation of kinetic energy is expressed as

$$\int_{t_1}^{t_2}\delta T dt=\int_{t_1}^{t_2}\int_{-h/2}^{h/2}\iint_A \rho\Big(\frac{\partial U}{\partial t}\frac{\partial \delta U}{\partial t}+\frac{\partial V}{\partial t}\frac{\partial \delta V}{\partial t}+\frac{\partial W}{\partial t}\frac{\partial \delta W}{\partial t}\Big)(R+z)dA\,dz\,dt \tag{15}$$

Or, in the final form yields

$$\begin{aligned}\int_{t_1}^{t_2}\delta T=\int_{t_1}^{t_2}\int_{-h/2}^{h/2}\iint_A\Big[&\rho\Big(-\frac{\partial^2 u_0}{\partial t^2}+z\frac{\partial^3 w}{\partial x\partial t^2}+\psi_1\frac{\partial^3\phi}{\partial x\partial t^2}\Big)\\&\Big(\delta u_0-z\frac{\partial\delta w}{\partial x}-\psi_1\frac{\partial\delta\phi}{\partial x}\Big)-\rho\Big(\frac{\partial^2 v_0}{\partial t^2}-\frac{z}{R+z}\frac{\partial^3 w}{\partial\theta\partial t^2}\\&-\frac{\psi_1}{R+z}\frac{\partial^3\phi}{\partial\theta\partial t^2}\Big)\Big(\delta v_0-\frac{z}{R+z}\frac{\partial\delta w}{\partial\theta}-\frac{\psi_1}{R+z}\frac{\partial\delta\phi}{\partial\theta}\Big)-\\&\rho\Big(\frac{\partial^2 w}{\partial t^2}+\frac{\partial^2\phi}{\partial t^2}+\psi_2\frac{\partial^2\chi}{\partial t^2}\Big)\Big(\delta w+\delta\phi+\psi_2\,\delta\chi\Big)\Big]\\&(R+z)dA\,dz\,dt\end{aligned} \tag{16}$$

The integration constants in Eq. (16) are presented in appendix A. In addition, the work due to reaction of Pasternak's foundation is assumed as

$$\begin{aligned}\delta W=&\iint_A\{(-K_w W+G(\nabla^2 W))\delta W=\\&\iint_A\Bigg\{\delta w\Big[-K_w w-K_w\phi+G\frac{\partial^2 w}{\partial x^2}+\\&G\frac{1}{(R+h/2)^2}\frac{\partial^2 w}{\partial\theta^2}\Big)+G\frac{\partial^2\phi}{\partial x^2}+\\&G\frac{1}{(R+h/2)^2}\frac{\partial^2\phi}{\partial\theta^2}\Big]+\delta\phi\Big[(-K_w w-K_w\phi+\\&G\frac{\partial^2 w}{\partial x^2}+G\frac{1}{(R+h/2)^2}\frac{\partial^2 w}{\partial\theta^2}+G\frac{\partial^2\phi}{\partial x^2}+\\&G\frac{1}{(R+h/2)^2}\frac{\partial^2\phi}{\partial\theta^2}\Big]d\theta dx\Bigg\}\end{aligned} \tag{17}$$

In which K_w and G are spring and shear parameters of foundation. Now, by separating of variables in Hamilton's principle from Eq. (12), the five governing equations of motion are derived as

$$\begin{aligned}\delta u_0:\;&a_1\frac{\partial^2 u_0}{\partial x^2}+a_2\frac{\partial^2 u_0}{\partial\theta^2}+a_3\frac{\partial^2 v_0}{\partial x\partial\theta}+a_4\frac{\partial\chi}{\partial x}+a_5\frac{\partial w}{\partial x}\\&+a_6\frac{\partial^3 w}{\partial x^3}+a_7\frac{\partial^3 w}{\partial x\partial\theta^2}+a_8\frac{\partial\phi}{\partial x}+a_9\frac{\partial^3\phi}{\partial x^3}+\\&a_{10}\frac{\partial^3\phi}{\partial x\partial\theta^2}=a_{11}\frac{\partial^2 u_0}{\partial t^2}+a_{12}\frac{\partial^4 u_0}{\partial t^2\partial x^2}+a_{13}\frac{\partial^4 u_0}{\partial t^2\partial\theta^2}\\&+a_{14}\frac{\partial^3 w}{\partial t^2\partial x}+a_{15}\frac{\partial^5 w}{\partial t^2\partial x^3}+a_{16}\frac{\partial^5 w}{\partial t^2\partial\theta^2\partial x}+\\&a_{17}\frac{\partial^3\phi}{\partial t^2\partial x}+a_{18}\frac{\partial^4\phi}{\partial t^2\partial x^2}+a_{19}\frac{\partial^5\phi}{\partial t^2\partial\theta^2\partial x}\end{aligned} \tag{18}$$

$$\begin{aligned}\delta v_0:\;&b_1\frac{\partial^2 u_0}{\partial x\partial\theta}+b_2 v_0+b_3\frac{\partial^2 v_0}{\partial\theta^2}+b_4\frac{\partial^2 v_0}{\partial x^2}+b_5\frac{\partial\chi}{\partial\theta}\\&+b_6\frac{\partial w}{\partial\theta}+b_7\frac{\partial^3 w}{\partial\theta^3}+b_8\frac{\partial^3 w}{\partial\theta\partial x^2}+b_9\frac{\partial\phi}{\partial\theta}+b_{10}\frac{\partial^3\phi}{\partial\theta^3}+\\&b_{11}\frac{\partial^3\phi}{\partial\theta\partial x^2}=b_{12}\frac{\partial^2 v_0}{\partial t^2}+b_{13}\frac{\partial^4 v_0}{\partial t^2\partial x^2}+b_{14}\frac{\partial^4 v_0}{\partial t^2\partial\theta^2}+\\&b_{15}\frac{\partial^3 w}{\partial t^2\partial\theta}+b_{16}\frac{\partial^5 w}{\partial t^2\partial x^2\partial\theta}+b_{17}\frac{\partial^5 w}{\partial t^2\partial\theta^3}+\\&b_{18}\frac{\partial^3\phi}{\partial t^2\partial\theta}+b_{19}\frac{\partial^5\phi}{\partial t^2\partial x^2\partial\theta}+b_{20}\frac{\partial^5\phi}{\partial t^2\partial\theta^3}\end{aligned} \tag{19}$$

$$\begin{aligned}\delta\chi:\;&c_1\frac{\partial u_0}{\partial x}+c_2\frac{\partial v_0}{\partial\theta}+c_3\chi+c_4\frac{\partial^2\chi}{\partial x^2}+c_5\frac{\partial^2\chi}{\partial\theta^2}\\&+c_6 w+c_7\frac{\partial^2 w}{\partial\theta^2}+c_8\frac{\partial^2 w}{\partial x^2}+c_9\phi+c_{10}\frac{\partial^2\phi}{\partial\theta^2}+\\&c_{11}\frac{\partial^2\phi}{\partial x^2}=c_{12}\frac{\partial^2\chi}{\partial t^2}+c_{13}\frac{\partial^4\chi}{\partial t^2\partial x^2}+c_{14}\frac{\partial^4\chi}{\partial t^2\partial\theta^2}+\\&c_{15}\frac{\partial^2 w}{\partial t^2}+c_{16}\frac{\partial^4 w}{\partial t^2\partial x^2}+c_{17}\frac{\partial^4 w}{\partial t^2\partial\theta^2}+c_{18}\frac{\partial^2\phi}{\partial t^2}+\\&c_{19}\frac{\partial^4\phi}{\partial t^2\partial x^2}+c_{20}\frac{\partial^4\phi}{\partial t^2\partial\theta^2}\end{aligned} \tag{20}$$

$$\begin{aligned}\delta w:\;&d_1\frac{\partial u_0}{\partial x}+d_2\frac{\partial^3 u_0}{\partial x\partial\theta^2}+d_3\frac{\partial^3 u_0}{\partial x^3}+d_4\frac{\partial v_0}{\partial\theta}\\&+d_5\frac{\partial^3 v_0}{\partial\theta^3}+d_6\frac{\partial^3 v_0}{\partial\theta\partial x^2}+d_7\chi+d_8\frac{\partial^2\chi}{\partial\theta^2}+\\&d_9\frac{\partial^2\chi}{\partial x^2}+d_{10}w+d_{11}\frac{\partial^2 w}{\partial x^2}+d_{12}\frac{\partial^2 w}{\partial\theta^2}+\\&d_{13}\frac{\partial^4 w}{\partial\theta^4}+d_{14}\frac{\partial^4 w}{\partial x^2\partial\theta^2}+d_{15}\frac{\partial^4 w}{\partial x^4}+d_{16}\phi\\&+d_{17}\frac{\partial^2\phi}{\partial x^2}+d_{18}\frac{\partial^2\phi}{\partial\theta^2}+d_{19}\frac{\partial^4\phi}{\partial\theta^4}+\\&d_{20}\frac{\partial^4\phi}{\partial x^2\partial\theta^2}+d_{21}\frac{\partial^4\phi}{\partial x^4}=d_{22}\frac{\partial^3 u_0}{\partial t^2\partial x}+\\&+d_{26}\frac{\partial^5 v_0}{\partial t^2\partial x^2\partial\theta}+d_{23}\frac{\partial^5 u_0}{\partial t^2\partial x^3}+\\&d_{24}\frac{\partial^5 u_0}{\partial t^2\partial\theta^2\partial x}+d_{25}\frac{\partial^3 v_0}{\partial t^2\partial\theta}+\\&d_{26}\frac{\partial^5 v_0}{\partial t^2\partial x^2\partial\theta}+d_{27}\frac{\partial^5 v_0}{\partial t^2\partial\theta^3}+d_{28}\frac{\partial^2\chi}{\partial t^2}\\&+d_{29}\frac{\partial^4\chi}{\partial t^2\partial x^2}+d_{30}\frac{\partial^4\chi}{\partial t^2\partial\theta^2}+d_{31}\frac{\partial^2 w}{\partial t^2}\\&+d_{32}\frac{\partial^4 w}{\partial t^2\partial x^2}+d_{33}\frac{\partial^4 w}{\partial t^2\partial\theta^2}+d_{34}\frac{\partial^6 w}{\partial t^2\partial x^4}\\&+d_{35}\frac{\partial^6 w}{\partial t^2\partial x^2\partial\theta^2}+d_{36}\frac{\partial^6 w}{\partial t^2\partial\theta^4}+d_{37}\frac{\partial^2\phi}{\partial t^2}\\&+d_{38}\frac{\partial^4\phi}{\partial t^2\partial x^2}+d_{39}\frac{\partial^4\phi}{\partial t^2\partial\theta^2}+d_{40}\frac{\partial^6\phi}{\partial t^2\partial x^4}\\&+d_{41}\frac{\partial^6\phi}{\partial t^2\partial x^2\partial\theta^2}+d_{42}\frac{\partial^6\phi}{\partial t^2\partial\theta^4}\end{aligned} \tag{21}$$

$$\delta\phi: e_1\frac{\partial u_0}{\partial x}+e_2\frac{\partial^3 u_0}{\partial x\partial\theta^2}+e_3\frac{\partial^3 u_0}{\partial x^3}+e_4\frac{\partial v_0}{\partial\theta}+e_5\frac{\partial^3 v_0}{\partial\theta\partial x^2}+e_6\frac{\partial^3 v_0}{\partial\theta^3}+e_7\,\chi+e_8\frac{\partial^2\chi}{\partial\theta^2}+e_9\frac{\partial^2\chi}{\partial x^2}+e_{10}\,w+e_{11}\frac{\partial^2 w}{\partial x^2}+e_{12}\frac{\partial^2 w}{\partial\theta^2}+e_{13}\frac{\partial^4 w}{\partial\theta^4}+e_{14}\frac{\partial^4 w}{\partial x^2\partial\theta^2}+e_{15}\frac{\partial^4 w}{\partial x^4}+e_{16}\phi+e_{17}\frac{\partial^2\phi}{\partial x^2}+e_{18}\frac{\partial^2\phi}{\partial\theta^2}+e_{19}\frac{\partial^4\phi}{\partial\theta^4}+e_{20}\frac{\partial^4\phi}{\partial x^2\partial\theta^2}+e_{21}\frac{\partial^4\phi}{\partial x^4}=e_{22}\frac{\partial^3 u_0}{\partial t^2\partial x}+e_{23}\frac{\partial^5 u_0}{\partial t^2\partial x^3}+e_{24}\frac{\partial^5 u_0}{\partial t^2\partial\theta^2\partial x}+e_{25}\frac{\partial^3 v_0}{\partial t^2\partial\theta}+e_{26}\frac{\partial^5 v_0}{\partial t^2\partial x^2\partial\theta}+e_{27}\frac{\partial^5 v_0}{\partial t^2\partial\theta^3}+e_{28}\frac{\partial^2\chi}{\partial t^2}+e_{29}\frac{\partial^4\chi}{\partial t^2\partial x^2}+e_{30}\frac{\partial^4\chi}{\partial t^2\partial\theta^2}+e_{31}\frac{\partial^2 w}{\partial t^2}+e_{32}\frac{\partial^4 w}{\partial t^2\partial x^2}+e_{33}\frac{\partial^4 w}{\partial t^2\partial\theta^2}+e_{34}\frac{\partial^6 w}{\partial t^2\partial x^4}+e_{35}\frac{\partial^6 w}{\partial t^2\partial x^2\partial\theta^2}+e_{36}\frac{\partial^6 w}{\partial t^2\partial\theta^4}+e_{37}\frac{\partial^2\phi}{\partial t^2}+e_{38}\frac{\partial^4\phi}{\partial t^2\partial x^2}+e_{39}\frac{\partial^4\phi}{\partial t^2\partial\theta^2}+e_{40}\frac{\partial^6\phi}{\partial t^2\partial x^4}+e_{41}\frac{\partial^6\phi}{\partial t^2\partial x^2\partial\theta^2}+e_{42}\frac{\partial^6\phi}{\partial t^2\partial\theta^4} \tag{22}$$

Now, it can be noted that Eqs. (18)-(22) are equations of motion of FG cylindrical nano shell based on the sinusoidal shear and normal deformation theory and nonlocal theory with thickness stretching effect.

3. Solution procedure and numerical results

Solution procedure is developed in this section for a simply-supported boundary condition. The displacement field and electric potential distribution are assumed based on trigonometric functions for simply-supported boundary conditions as follows

$$\begin{aligned} u_0 &= u_{0mn}\cos(\frac{m\pi x}{L})\cos(n\theta)\\ v_0 &= v_{0mn}\sin(\frac{m\pi x}{L})\sin(n\theta)\\ w &= w_{mn}\sin(\frac{m\pi x}{L})\cos(n\theta)\\ \phi &= \phi_{mn}\sin(\frac{m\pi x}{L})\cos(n\theta)\\ \chi &= \chi_{mn}\sin(\frac{m\pi x}{L})\cos(n\theta) \end{aligned} \tag{23}$$

In which $\{d\}=\{u_{0mn}\ v_{0mn}\ \chi_{mn}\ w_{mn}\ \phi_{mn}\}^T$ is unknown vector, m and n represent the axial and circumferential wave numbers, respectively. By substituting Eq. (23) into equations of motion (18) - (22), the governing equations are written in the matrix form as follows

$$\{K\}\left\{d\right\}+\{M\}\left\{\ddot{d}\right\}=0 \tag{24}$$

Where

$$\{d\}=\{d_0\}\ e^{i\omega t} \tag{25}$$

Now, by substituting Eq. (25) into (24), we will have

$$(\{K\}-\omega^2\{M\})\{d_0\}=0 \tag{26}$$

Where ω stands for natural frequency, $\{d_0\}=\{u_{0mn}\ v_{0mn}\ \chi_{mn}\ w_{mn}\ \phi_{mn}\}^T$ is displacement amplitude vector. The natural frequencies of the FG cylindrical nanoshell is derived using determinant of characteristic equation (Eq. (26)).

The natural frequencies are calculated in terms of significant parameters of the problem such as dimensionless length scale parameters, distribution of properties of nanoshell components, dimensionless geometric parameters such as length to radius ratio L/R, and thickness to radius ratio h/R, circumferential n and axial wave numbers m. As mentioned before, by setting the material length parameter to zero, equations will be obtained on the basis of the classical theory. The FG cylindrical nanoshell is made of aluminum (Al) and ceramic (Sic) with following material properties (Tadi Beni *et al*. 2015)

$$AL: E=70\ Gpa,\ \rho=2702\ (kg/m^3)$$
$$Sic: E=427\ Gpa,\ \rho=3100\ (kg/m^3)$$

Before presentation of complete numerical results, a comprehensive comparative study is performed for validation of our formulation and corresponding numerical results. Therefore, the accuracy of results for an isotropic homogeneous cylindrical nanoshell is examined by setting N = 0. The material properties used in this section are considered as follows (Alibeigloo and Shaban 2013)

$$E=1.06\ Tpa,\ \upsilon=0.3,\ R=2\,nm,\ L/R=1,$$
$$\rho=2300\,kg/m^3,\ m=1$$

The dimensionless natural frequency based on (Tadi Beni *et al.* 2015) is defined as $\Omega=R\,\omega\sqrt{\rho/E}$ Shown in Fig. 2 is comparison of dimensionless natural frequencies of FG cylindrical nanoshell in terms of nonlocal parameter for various inhomogeneous indexes. The numerical results indicate that with increase of nonlocal parameter, the stiffness of cylindrical nanoshell is decreased that leads to decrease of the natural frequencies. It can be concluded that decrease of natural frequencies with increase of nonlocal parameter is in accordance with references Alibeigloo and Shaban (2013) and Tadi Beni *et al.* (2015). In addition, it can be concluded that with increase of ratio h/R, the natural frequencies are increased. One can conclude that with

increase of thickness to radius ratio, the bending stiffness of nanoshell is increased and consequently the natural frequencies are increased significantly.

Table 1 lists comparison of the non-dimensional fundamental natural frequencies of isotropic nanoshell in terms of circumferential wave numbers based on first order shear deformation theory and 3D solution proposed by Alibeigloo and Shaban (2013) and Tadi Beni *et al.* (2015), respectively. This comparison indicates that the numerical results in this paper are in good agreement. One can conclude that employing thickness stretching effect leads to significant improvement of previous lower order theories. In this stage, the full numerical results of functionally graded nanoshell are presented. Fig. 3 shows the variation of dimensionless of natural frequency $(\Omega = R\omega\sqrt{\rho_m / E_m})$ in terms of nonlocal parameter to thickness dimensionless ratio L_1 / h in terms of various inhomogeneous indexes N. It can be concluded that with increase of inhomogeneous index N, the natural frequencies are significantly increased. It is noticeable that N = 0 is corresponding to a shell made of pure aluminum shell and $N = \infty$ to a pure ceramic shell. One can conclude that with increase of inhomogeneous index N, the stiffness of shell is increased that leads to increase of natural frequencies.

Table 2 lists fundamental natural frequencies of nanoshell in terms of nonlocal parameter for various length to radius ratio L/R. It is concluded that with increase of nonlocal parameter, the stiffness of structure is decreased and consequently the natural frequencies are decreased significantly. In addition, it can be observed that with increasing the ratio L/R the natural frequencies are decreased significantly. It is concluded that with increase of length to radius ratio L/R, the stiffness is decreased.

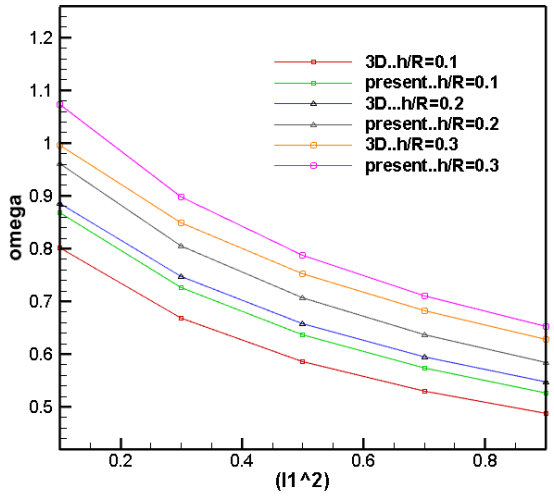

Fig. 2 Comparison of fundamental natural frequencies of FG nanoshell in terms of various nonlocal parameters and ratio h/R with 3D results of Alibeigloo and Shaban (2013)

Table 1 Comparison of fundamental natural frequencies of FG nanoshell in terms of various circumferential wave numbers and thickness to radius ratio h/R with Alibeigloo and Shaban (2013) and Tadi Beni *et al.* (2015)

(L/R=1,R=2nm) h/R	n	Alibeigloo and Shaban (2013)	Tadi Beni et al. (2015)	Present study
0.1	1	0.913	0.933	0.9784
	2	0.762	0.776	0.8197
	3	0.699	0.713	0.7464
0.2	1	0.993	1.048	1.0846
	2	0.936	0.971	1.0092
	3	0.999	1.052	1.0903
0.3	1	1.112	1.181	1.2109
	2	1.116	1.162	1.2057
	3	1.245	1.330	1.3880

Table 2 Fundamental natural frequencies of nanoshell in terms of nonlocal parameter for various length to radius ratio L/R

(h/R=0.1,R=2nm,N=2) L/R	L_1	Ω_{11}
4	0.1	0.82445
	0.2	0.8195
	0.5	0.78722
	1	0.69693
8	0.1	0.5022
	0.2	0.50005
	0.5	0.48567
	1	0.44292
12	0.1	0.42385
	0.2	0.42216
	0.5	0.41088
	1	0.37692
20	0.1	0.38281
	0.2	0.38135
	0.5	0.37156
	1	0.34189

Fig. 4 shows the variation of dimensionless natural frequency in terms of nonlocal parameter to thickness dimensionless ratio L_1 / h for various axial wave numbers m. It can be concluded that the natural frequencies are decreased with increase of nonlocal parameter. In addition, the for small nonlocal parameter to thickness dimensionless ratio L_1 / h, the natural frequencies are decreased with increase of axial wave number.

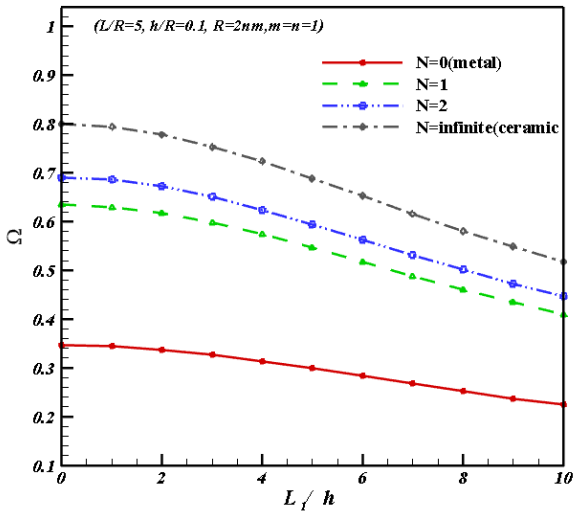

Fig. 3 Variation of dimensionless natural frequency in terms of nonlocal parameter to thickness ratio L_1/h for various inhomogeneous indexes

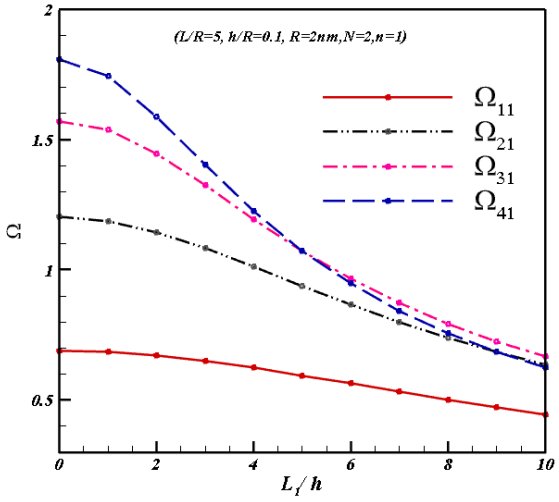

Fig. 4 Variation of dimensionless natural frequency in terms of nonlocal parameter to thickness ratio L_1/h for various axial wave numbers

Fig. 5 shows the variation of dimensionless natural frequency in terms of length to radius ratio L/R for various axial wave numbers m. It can be concluded that with increase of ratio L/R, the natural frequency decreases.

Fig. 6 shows the variation of dimensionless natural frequency in terms of length to radius ratio L/R for various nonlocal parameters. It can be concluded that with increase of length to radius ratio L/R and nonlocal parameter, stiffness of shell decreases that leads to significant decrease of natural frequencies.

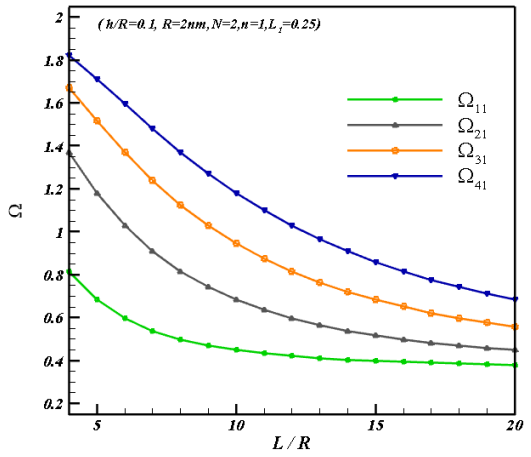

Fig. 5 Variation of dimensionless natural frequency in terms of length to radius ratio L/R for various axial wave numbers

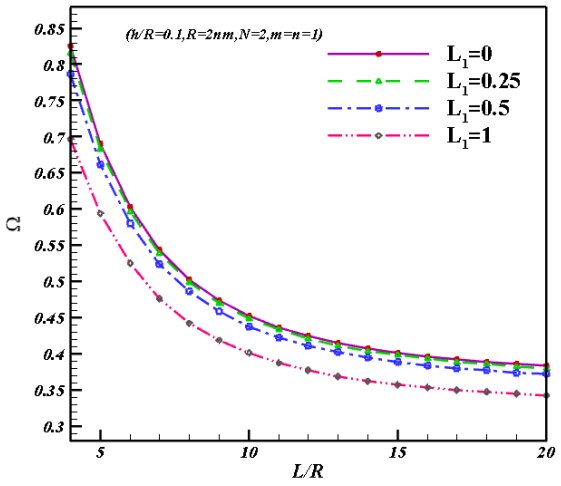

Fig. 6 Variation of dimensionless natural frequency in terms of length to radius ratio L/R for various nonlocal parameters

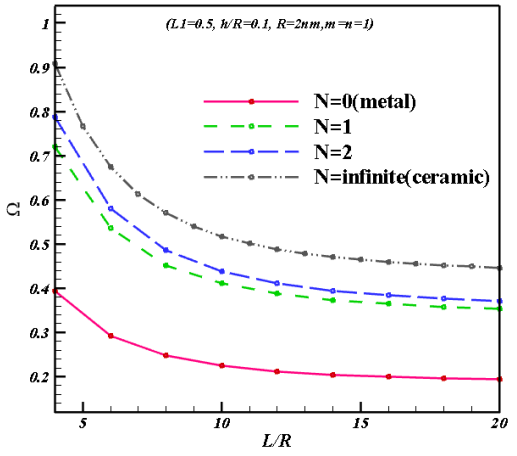

Fig. 7 Variation of dimensionless natural frequency in terms of length to radius ratio L/R for various inhomogeneous indexes

Fig. 7 shows the variation of dimensionless natural frequency in terms of length to radius ratio L/R for various inhomogeneous indexes N. The numerical results indicate that the natural frequencies are decreased with increase of length to radius ratio L/R and decrease of inhomogeneous index. One can conclude that the stiffness of functionally graded nanoshell is increased with increase of inhomogeneous index.

Figs. 8 and 9 illustrate the effect of axial and circumferential wave numbers as well as thickness to radius ratio h/R on the dimensionless natural frequency, respectively. The other data are assumed as: $L_1 = 0.25$, N = 2. Figure 8 shows that the natural frequencies are increased significantly with increase of axial wave number, m and thickness to radius ratio h/R.

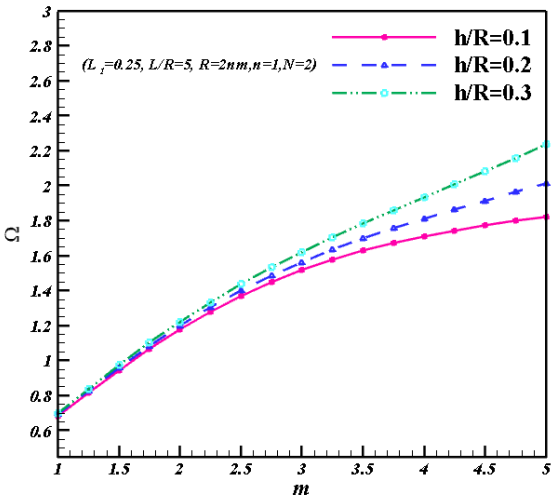

Fig. 8 Variation of dimensionless natural frequencies of nanoshell in terms of axial wave number for various thickness to radius ratio

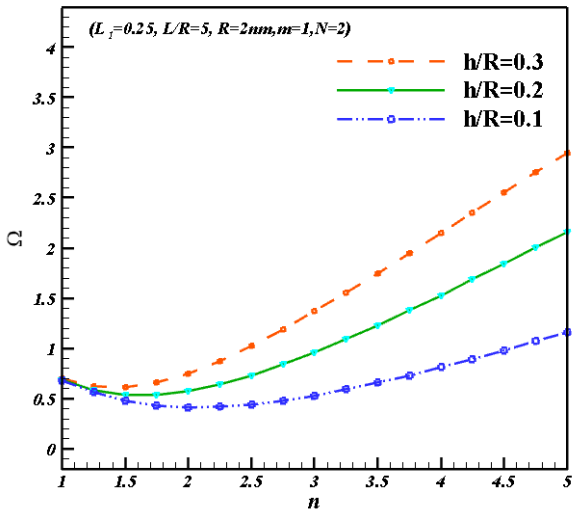

Fig. 9 Variation of dimensionless natural frequencies of nanoshell in terms of circumferential wave number for various thickness to radius ratio

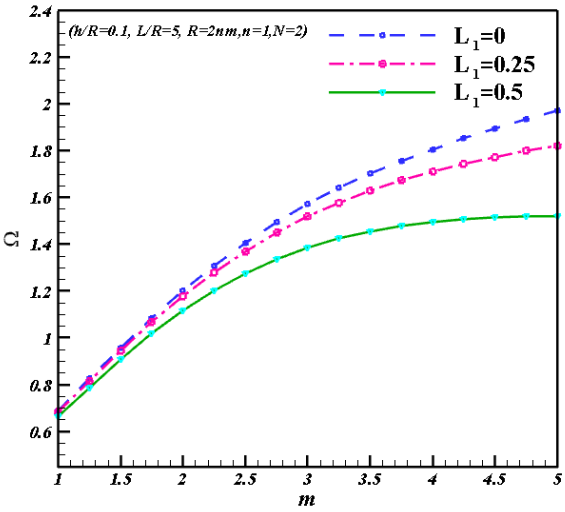

Fig. 10 Variation of dimensionless natural frequencies of nanoshell in terms of axial wave number for various nonlocal parameter

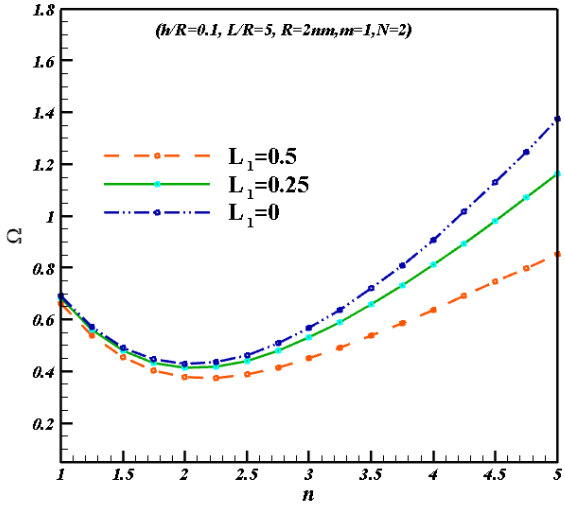

Fig. 11 Variation of dimensionless natural frequencies of nanoshell in terms of circumferential wave number for various nonlocal parameter

It is concluded that for higher modes of vibration (higher values of axial mode number m), higher natural frequencies are required. In addition, with increase of thickness to radius ratio h/R, the stiffness is increased that needs to higher values of natural frequencies.

Fig. 9 shows that the natural frequencies are decreased for increase of circumferential wave number to minimum one and then are increased with increase of circumferential wave number. The minimum natural frequencies are depending on the thickness to radius ratio h/R. The corresponding circumferential wave number for minimum natural frequencies is decreased with increase of thickness to radius ratio h/R.

Figs. 10 and 11 show the effect of axial and circumferential wave numbers as well as length scale parameter on the dimensionless natural frequency of cylindrical nano shell. The present numerical results are obtained for $h/R=0.1$, $N=2$. Both figures show that increase of nonlocal parameter leads to decrease of stiffness of nanoshell and consequently decrease of natural frequencies. In addition, increase of axial wave number leads to increase of natural frequencies while increase of circumferential wave number firstly leads to decrease of natural frequency and then increase of it. The minimum natural frequencies are occurred approximately for n=2.25.

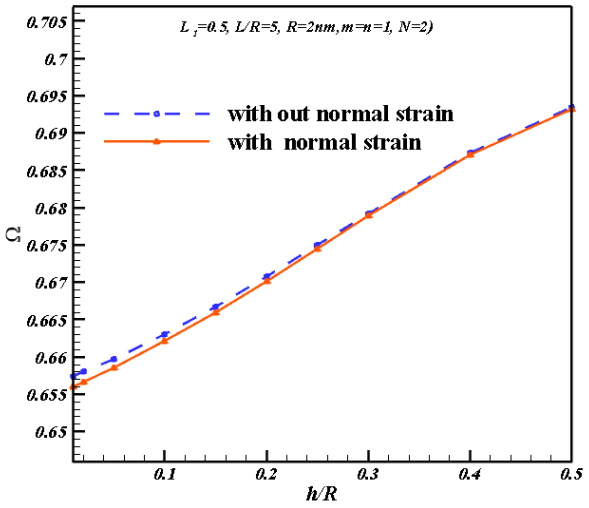

Fig. 12 Variation of dimensionless natural frequencies in terms of thickness to radius ratio h/R with and without thickness stretching effect

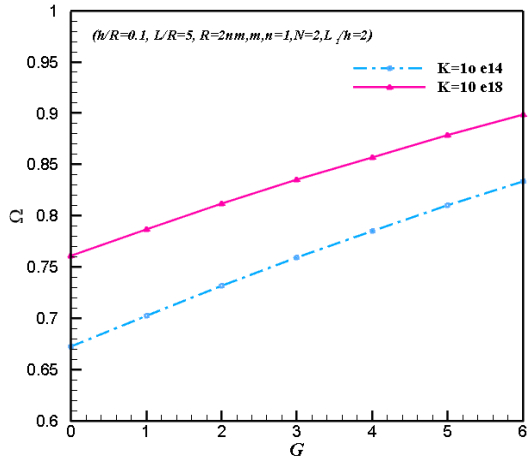

Fig. 13 Variation of dimensionless natural frequencies of nanoshell in terms of two parameters of Pasternak's foundation

Shown in Fig. 12 is variation of dimensionless natural frequencies in terms of thickness to radius ratio h/R with and without thickness stretching effect. The numerical results indicate that considering thickness stretching effect based on sinusoidal higher order shear and normal deformation theory leads to significant improvement of results rather than the case that ignores this effect.
The effect of two parameters of Pasternak's foundation is observed in Fig. 13. The numerical results indicate that the natural frequencies are increased significantly with increase of two parameters of Pasternak's foundation.

4. Conclusions

Free vibration analysis of a FG cylindrical nanoshell was studied in this work based on the sinusoidal higher-order shear and normal deformation theory and Eringen nonlocal elasticity theory. The thickness stretching effect and size dependency were accounted using the higher-order shear and normal deformation theory and Eringen nonlocal elasticity theory, respectively. Hamilton's principle was used for derivation of governing equations of motion. The governing equations of motion were solved for a simply supported boundary conditions based on the Navier technique. The comparative study was performed to study trueness and importance of the present theory. The natural frequencies were presented in terms of important input parameters such as nonlocal parameter, axial and circumferential wave numbers, some dimensionless geometric parameters such as length to radius and thickness to radius ratios. The main conclusions of the present paper are expressed as:

Comparison between the cases with and without thickness stretching effect indicates that accounting thickness stretching effect leads to more accurate results.

Increase of the nonlocal parameter based on Eringen nonlocal elasticity theory leads to decrease of stiffness of nanoshell and then decrease of natural frequencies of nanoshell.

Increase of length to radius L/R ratio and decrease of thickness to radius ratio h/R leads to decrease of stiffness of cylindrical nanoshell and then decrease of natural frequencies of nanoshell.

Change of axial and circumferential wave numbers leads to different behaviors of natural frequencies of cylindrical nanoshell. The numerical results indicates that increase of axial wave number leads to increase of natural frequencies while increase of circumferential wave number leads to decrease of natural frequencies for small values of this wave number and increase of natural frequencies for large values of wave number.

References

Ansari, R., Rouhi, H. and Rajabiehfard, R.. (2012), "Free vibration analysis of single-walled carbon nanotubes using semi-

analytical finite element", *Int J Comput Meth Eng Sci Mech*., **13**,1-8. https://doi.org/10.1080/15502287.2012.660234.

Ansari, R., Rouhi, H. and Sahmani, S. (2011),"Calibration of the analytical nonlocal shell model for vibrations of double-walled carbon nanotubes with arbitrary boundary conditions using molecular dynamics", *Int J Mech Sci*., **53**, 786-792. https://doi.org/10.1016/j.ijmecsci.2011.06.010..

Alibeigloo, A. and Shaban, M. (2013),"Free vibration analysis of carbon nanotubes by using three-dimensional theory of elasticity", *Acta Mech*., **224**(7), 1415-1427. https://doi.org/10.1007/s00707-013-0817-2.

Ansari, R., Sahmani, S. and Rouhi, H. (2011), "Rayleigh–Ritz axial buckling analysis of single-walled carbon nanotubes with different boundary conditions", *Phys. Lett. A*, **375** ,1255-1263. https://doi.org/10.1016/j.physleta.2011.01.046.

Arash, B and Wang, Q. (2012), "A review on the application of nonlocal elastic models in modeling of carbon nanotubes and graphenes", *Comput. Mater. Sci*., **51**, 303-313. https://doi.org/10.1007/978-3-319-01201-8_2.

Arefi, M and Zenkour, A.M. (2016), "Free vibration, wave propagation and tension analyses of a sandwich micro/nano rod subjected to electric potential using strain gradient theory", *Mater, Res, Express*., **3**, 115704. https://doi.org/10.1088/2053-1591/3/11/115704.

Arefi, M. and Zenkour, A.M. (2017a), "Thermo-electro-mechanical bending behavior of sandwich nanoplate integrated with piezoelectric face-sheets based on trigonometric plate theory", *Compos Struct*., **162**, 108-122. https://doi.org/10.1016/j.compstruct.2016.11.071.

Arefi, M., Kiani, M. and Zenkour, A.M. (2017b), "Size-dependent free vibration analysis of a three-layered exponentially graded nano-/micro-plate with piezo magnetic face sheets resting on Pasternak's foundation via MCST", *Sandw. Struct. Mater.*, https://doi.org/10.1177/1099636217734279.

Arefi, M. and Zenkour, A.M. (2017c), "Size-dependent free vibration and dynamic analyses of piezo-electro-magnetic sandwich nanoplates resting on viscoelastic foundation", *Phys. B: Cond. Matter.*, **521**, 188-197. https://doi.org/10.1016/j.physb.2017.06.066.

Arefi, M. and Zenkour, A.M. (2017d), "Transient sinusoidal shear deformation formulation of a size-dependent three-layer piezo-magnetic curved nanobeam", *Acta. Mech.*, **228**(10), 3657-3674. https://doi.org/10.1007/s00707-017-1892-6.

Arefi, M. and Zenkour, A.M. (2019), "Influence of magneto-electric environments on size-dependent bending results of three-layer piezomagnetic curved nanobeam based on sinusoidal shear deformation theory", *J. Sandw. Struct. Mater.*, **21**(8), 2751-2778. https://doi.org/10.1177/1099636217723186.

Amiri, F., Millán, D., Shen, Y., Rabczuk, T. and Arroyo, M. (2014), "Phase-field modeling of fracture in linear thin shells", *Theor. Appl. Fract. Mech.*, **69**, 102-109., https://doi.org/10.1016/j.tafmec.2013.12.002

Areias, P., Rabczuk, T. and Msekh, M.A. (2016), "Phase-field analysis of finite-strain plates and shells including element Subdivision", *Comput. Method. Appl. M.*, **312**, 322-235. http://dx.doi.org/10.1016/j.cma.2016.01.020.

Baghani, M., MohammadSalehi, M. and Dabaghian, P.H. (2016), "Analytical couple-stress solution for size-dependent large-amplitude vibrations of FG tapered-nanobeams", *Solids Struct*., **13**(1). http://dx.doi.org/10.1590/1679-78252175.

Belkorissat, I., Ahmed Houari, M.S., Tounsi, A., Adda Bedia, E.A. and Mahmoud, S.R. (2015), "On vibration properties of functionally graded nano-plate using a new nonlocal refined four variable mode", *Steel Compos. Struct.*, **18**, 1063-1081. http://dx.doi.org/10.12989/scs.2015.18.4.1063.

Budarapu, P.R. Reinoso, J. and Paggi, M. (2017a), "Concurrently coupled solid shell-based adaptive multiscale method for fracture", *Comput. Method. Appl. M.*, **319**(1), 338-365. https://doi.org/10.1016/j.cma.2017.02.023.

Budarapu, P.R. and Rabczuk, T. (2017b), "Multiscale methods for fracture: A review". *J. Ind. Inst. Sci*., **97**(3), 339-376. https://doi.org/10.1007/s41745-017-0041-5.

Budarapu, P.R., Gracie, R., Yang, S.W., Zhuang, X. and Rabczuk, T. (2014), "Efficient Coarse Graining in Multiscale Modeling of Fracture", *Theor. Appl. Fract. Mech*., **69**, 126-143. https://doi.org/10.1016/j.tafmec.2013.12.004.

Chen, W.Q., Ying, J. and Yang, Q.D. (2008), "Free vibrations of transversely isotropic cylinders and cylindrical shells", *Pressure Vessel Technol*., **120**(4). https://doi.org/10.1115/1.2842338.

Duan, W.H., Wang, C.M. and Zhang, Y.Y. (2007), "Calibration of nonlocal scaling effect parameter for free vibration of carbon nanotubes by molecular dynamics", *J. Appl. Phys.*, **101**, 024305. https://doi.org/10.1063/1.2423140.

Daneshmand, F., Rafiei, M., Mohebpour, S. and Heshmati, M. (2013), "Stress and strain-inertia gradient elasticity in free vibration analysis of single walled carbon nanotubes with first order shear deformation shell theory", *Appl. Math. Model.,* **37**, 7983-8003. https://doi.org/10.1016/j.apm.2013.01.052.

Eringen, A.C. (1983), "On differential equations of nonlocal elasticity and solutions of screw dislocation and surface waves", *J. Appl. Phys*., **54**, 4703-4710. ttps://doi.org/10.1063/1.332803.

Gurtin, M.E. and Murdoch, A. (1975), "A continuum theory of elastic material surfaces", *Arch. Rat. Mech. Anal.*, **57**, 291-323. https://doi.org/10.1007/BF00261375.

Gurtin, M.E and Murdoch, A. (1978), "Surface stress in solids". *Int. J. Solids Struct.*, **14**, 431-440., .https://doi.org/10.1007/BF00261375

Gurtin, M.E., Issmüller, W.E and Larché, J. (1998), "A general theory of curved deformable interfaces in solids at equilibrium", *Philos. Mag.*, **78**(5), 1093-1109. https://doi.org/10.1080/01418619808239977.

Ghavanloo, E. and Fazelzadeh, A. (2013), "Nonlocal elasticity theory for radial vibration of nanoscale spherical shells", *Mech. A/Solids*, **41**, 37-42., https://doi.org/10.1016/j.euromechsol.2013.02.003,

Gholami, R., Darvizeh, A., Ansari, A. and Sadeghi, F. (2016), "Vibration and buckling of first-order shear deformable circular cylindrical micro-/nano-shells based on Mindlin's strain gradient elasticity theory", *Mech. -A/Solids*., **58**,76-88., https://doi.org/10.1016/j.euromechsol.2016.01.014.

Guo, H., Zhuang, X. and Rabczuk, T. (2019), "A deep collocation method for the bending analysis of kirchhoff plate", *Comput. Mater. Continu*., **59**, 433-456. doi:10.32604/cmc.2019.06660.

Hosseini Ghoytasi, I. and Golmohammadi, H. (2018), "Free vibration of deep curved FG nano-beam based on modified couple stress theory", *Steel Compos. Struct*., **26**(5), 607., https://doi.org/10.12989/scs.2018.26.5.607.

Javvaji, B., Budarapu, P.R., Paggi, M., Zhuang, X. and Rabczuk, T. (2018), "Fracture Properties of Graphene-Coated Silicon for Photovoltaics", *Adv. Theory. Simulation.*, **1**(12), 1800097, https://doi.org/10.1002/adts.201800097.

Koutsoumaris, C.C., *et al*. (2015), "Application of bi-Helmholtz nonlocal elasticity and molecular simulations to the dynamical response of carbon nanotubes", *AIP Publishing LLC*., **3**, 28-42., https://doi.org/10.1063/1.4938978.

Lam, D., Yang, F., Chong, A., Wang, J and Tong, P. (2003) ,"Experiments and theory in strain gradient elasticity", *J. Mech. Phys. Solids.*, **51**,1477-1508. https://doi.org/10.1016/S0022-5096(03)00053-X.

Li, C., Liu, J.J., Cheng, M. and Fan, X.L. (2017), "Nonlocal vibrations and stabilities in parametric resonance of axially moving viscoelastic piezoelectric nanoplate subjected to thermo-electro-mechanical forces", *Compos. Part B: Eng.*, **116**,

153-69., https://doi.org/10.1016/j.compositesb.2017.01.071.
Moradi-Dastjerdi, R., Pourasghar, A. and Foroutan, M. (2014), "Vibration analysis of functionally graded nanocomposite cylinders reinforced by wavy carbon nanotube based on mesh-free method". *Compos. Mater*., **48**(15)., https://doi.org/10.1177/0021998313491617.
Murmu, T., Adhikari, S and Wang, C.Y. (2011), "Torsional vibration of carbon nanotube–buckyball systems based on nonlocal elasticity theory". *Physica E*, **43**, 1276–1280., https://doi.org/10.1016/j.physe.2011.02.017.
Nguyen-Thanh, N., Zhou, K., Zhuang, X., Areias, P., Nguyen-Xuan, H., Bazilevs, Y and Rabczuk, T. (2017), "Isogeometric analysis of large-deformation thin shells using RHT-splines for multiple-patch coupling", *Comput. Method. Appl. M*., **316**, 1157-1178., http://dx.doi.org/10.1016/j.cma.2016.12.002.
Pourasghar, A. and Chen, Z. (2016), "Thermoelastic response of CNT reinforced cylindrical panel resting on elastic foundation using theory of elasticity*", Compos. Part B Eng.*, **99,** 436-444. https://doi.org/10.1016/j.compositesb.2016.06.028.
Pradhan, S.C and Phadikar, J.K. (2009), "Small scale effect on vibration of embedded multilayered graphene sheets based on nonlocal continuum models", *Phys. Lett*., **373**, 1062-1069. https://doi.org/10.1016/j.physleta.2009.01.030.
Reddy, J. (2007), "Nonlocal theories for bending, buckling and vibration of beams", *Int J Eng Sci*., **45,** 288-307., https://doi.org/10.1016/j.ijengsci.2007.04.004.
Rabczuk, T., Gracie, R., Song, J.H. and Belytschko, T. (2010), "Immersed particle method for fluid–structure interaction", *Numer, Method Eng*., **81**, 48-71. 10.1002/nme.2670, 2010.
Rabczuk, T., Areias, P.M.A. and Belytschko, T. (2007), "A meshfree thin shell method for non-linear dynamic fracture", *Int. J. Numer. Meth. Eng.*, **72**, 524-548. https://doi.org/10.1002/nme.2013.
Shojaeefard, M.H., Mahinzare, M., Safarpour, H., Ghadiri, M. and Googarchin, H. (2018), "Free vibration of an ultra-fast-rotating induced cylindrical nano-shell resting on a Winkler foundation under thermo-electro-magneto-elastic condition", *Appl. Math. Model.,* **61**, 255-279. https://doi.org/10.1016/j.apm.2018.04.015.
Shaat, M and Abdelkefi, A. (2017), "New insights on the applicability of Eringen's nonlocal theory", *Int J Mech Sci*., **121**, 67-75., https://doi.org/10.1016/j.ijmecsci.2016.12.013.
She, G.L., Yuan, F.G., Ren, Y.R. and Xiao, W.S. (2017), "On buckling and postbuckling behavior of nanotubes", *Int. J. Eng. Sci*., **121**, 130-142. https://doi.org/10.1016/j.ijmecsci.2016.12.013.
Safaei, B., Moradi-Dastjerdi, R., Qin, Z.H. and Chu, F. (2018), "Frequency-dependent forced vibration analysis of nanocomposite sandwich plate under thermo-mechanical loads", *Compos. Part B Eng*., **18**, 148-176. https://doi.org/10.1016/j.compositesb.2018.10.049.
Salehipour, H., Nahvi, H. and Shahidi, A.R. (2015), "Exact closed-form free vibration analysis for functionally graded micro/nano plates based on modified couple stress and three-dimen-sional elasticity theories", *Compos. Struct*., **124**, 283-291. https://doi.org/10.1016/j.compstruct.2015.01.015.
Soleimani, I., Tadi Beni, Y. and Dehkordi, M.B. (2018), "Finite element vibration analysis of nanoshell based on new cylindrical shell element", *Struct. Eng. Mech.*, **65**(1), 33-41. https://doi.org/10.12989/sem.2018.65.1.033.
Tadi Beni, Y. (2016b), "Size-dependent electro mechanical bending, buckling, and free vibration analysis of functionally graded piezoelectric nanobeams", *J. Intel. Mat. Syst. Str.*, **27**, 2199-2215. https://doi.org/10.1177/1045389X15624798.
Tadi Beni, Y. (2016c), "Size-dependent analysis of piezoelectric nanobeams including electro-mechanical coupling", *Mech. Res. Commun*., **75**, 67-80. https://doi.org/10.1016/j.mechrescom.2016.05.011.
Tadi Beni, Y., Mehralian, F. and Razavi, H. (2015), "Free vibration analysis of size-dependent shear deformable functionally graded cylindrical shell on the basis of modified couple stress theory", *Compos. Struct.*, **120**, 65-106. https://doi.org/10.1016/j.compstruct.2014.09.065.
Wang, Q. (2005), "Wave propagation in carbon nanotubes via nonlocal continuum mechanics", *J. Appl. Phys.*, **98**, 124-130. https://doi.org/10.1063/1.2141648 .
Wang, Y.G., Lin, W.H. and Liu, N. (2013), "Large amplitude free vibration of size-dependent circular micro-plates based on the modified couple stress theory", *Int. J. Mech. Sci*., **71**, 51-57. https://doi.org/10.1016/j.ijmecsci.2013.03.008.
Wang, K., Wang, B. and Kitamura, T. (2015), "A review on the application of modified continuum models in modeling and simulation of nanostructures", *Acta Mech. Sinica*, **32**, 83-100. https://doi.org/10.1007/s10409-015-0508-4.
Xiang, H.J. and Yang, J. (2008), "Free and forced vibration of a laminated FGM Timoshenko beam of variable thickness under heat conduction", *Compos Part B-.Eng.*, **39**(2), 292-303., https://doi.org/10.1016/j.compositesb.2007.01.005.
Yildirm V. (1999), "A numerical study on the free vibration of symmetric cross-ply laminated cylindrical helical springs", *Appl. Mech.*, 66, 1040-1043. http://dx.doi:10.1115/1.2791780.
Yang, F., Chong, A., Lam, D. and Tong, P. (2002), "Couple stress based strain gradient theory for elasticity", *Int. J. Solids Struct*., **39**, 2731-2743. https://doi.org/10.1016/S0020-7683(02)00152-X.
Yan, Z. and Jiang, L.Y. (2012), "Vibration and buckling analysis of a piezoelectric nanoplate considering surface effects and in-plane constraints", *Math.. Phys. Eng. Sci.*, https://doi.org/10.1098/rspa.2012.0214
Zhu, C.S., Fang, X.Q., Liu, J.X and Li, H.Y. (2017), "Surface energy effect on nonlinear free vibration behavior of orthotropic piezoelectric cylindrical nano-shells", *Mech. - A/Solids*, **66**, 423-432. https://doi.org/10.1016/j.euromechsol.2017.08. 001.
Zeighampour, H. and Tadi Beni, Y. (2014), "Size-dependent vibration of fluid-conveying double-walled carbon nanotubes using couple stress shell theory", *Phys. E*, **61**, 28-39. https://doi.org/10.1016/j.physe.2014.03.011.
Zhang, Y., Wang, C. and Tan, V. (2009), "Assessment of Timoshenko beam models for vibrational behavior of single-walled carbon nanotubes using molecular dynamics", *Adv. Appl. Math. Mech*., **1**, 89-106. https://doi.org/10.1016/j.ijengsci.2007.04.004.
Zeighampour, H. and Tadi Beni, Y. (2015), "A shear deformable cylindrical shell model based on couple stress theory", *Arch. Appl. Mech*., **85**, 539-553. https://doi.org/10.1007/s00419-014-0929-8.
Zenkour, A.M. (2013), "Bending of FGM plates by a simplified four-unknown shear and normal deformations theory", *Int. J. Appl. Mech*., **5**, 1-15,. https://doi.org/10.1142/S1758825113500208.
Zenkour, A.M. (2013), "A simple four-unknown refined theory for bending analysis of functionally graded plates", *Appl. Math. Model*., **37**, 9041-9051., https://doi.org/10.1016/j.apm.2013.04.022.

CC

Appendix A: Unknown constants in the equations of motion

$$I_{ij}=\int_{-h/2}^{h/2}\rho\frac{z^i}{(R+z)^j}dz\ ,\ J_{ij}=\int_{-h/2}^{h/2}\rho\frac{\psi_1 z^i}{(R+z)^j}dz$$

$$L_{ij}=\int_{-h/2}^{h/2}\rho\frac{\psi_2 z^i}{(R+z)^j}dz\ ,\ K_{ij}=\int_{-h/2}^{h/2}\rho\frac{(\psi_2)^2 z^i}{(R+z)^j}dz$$

$$S_{ij}=\int_{-h/2}^{h/2}\rho\frac{(\psi_1)^2 z^i}{(R+z)^j}dz$$

$$N_{ij}^k=\int_{-h/2}^{h/2}\rho\frac{\sigma_{ij}}{(R+z)^k}dz\ ,\ i,j=x,\theta\quad k,l=1,2,,...$$

$$M_{ij}^k=\int_{-h/2}^{h/2}\rho\frac{\sigma_{ij}z}{(R+z)^k}dz\ ,\ E_{ij}^k=\int_{-h/2}^{h/2}\rho\frac{\sigma_{ij}z^2}{(R+z)^k}dz$$

$$A_{ij}^{kl}=\int_{-h/2}^{h/2}\rho\frac{\sigma_{ij}\psi_1 z^k}{(R+z)^l}dz\ ,\ B_{ij}^{kl}=\int_{-h/2}^{h/2}\rho\frac{\sigma_{ij}\psi_2 z^k}{(R+z)^l}dz$$

$$C_{ij}^{kl}=\int_{-h/2}^{h/2}\rho\frac{\sigma_{ij}z^k}{(R+z)^l}\frac{\partial\psi_1}{\partial z}dz\,,D_{ij}^{kl}=\int_{-h/2}^{h/2}\rho\frac{\sigma_{ij}z^k}{(R+z)^l}\frac{\partial\psi_2}{\partial z}dz$$

$$F_{ij}=\int_{-h/2}^{h/2}\lambda\frac{z^i}{(R+z)^j}dz,\quad i,j=1,2,...$$

$$H_{ij}=\int_{-h/2}^{h/2}\lambda\frac{\psi_1 z^i}{(R+z)^j}dz\,,G_{ij}=\int_{-h/2}^{h/2}\lambda\frac{\psi_2 z^i}{(R+z)^j}dz$$

$$Q_{ij}=\int_{-h/2}^{h/2}\lambda\frac{z^i}{(R+z)^j}\frac{\partial\psi_2}{\partial z}dz\,,P_{ij}=\int_{-h/2}^{h/2}\lambda\frac{z^i}{(R+z)^j}\frac{\partial\psi_1}{\partial z}dz$$

$$\hat{H}_{ij}=\int_{-h/2}^{h/2}\lambda\frac{\psi_1 z^i}{(R+z)^j}\frac{\partial\psi_2}{\partial z}dz\,,\hat{G}_{ij}=\int_{-h/2}^{h/2}\lambda\frac{\psi_2 z^i}{(R+z)^j}\frac{\partial\psi_2}{\partial z}dz$$

$$\hat{Q}_{ij}=\int_{-h/2}^{h/2}\lambda\frac{z^i}{(R+z)^j}(\frac{\partial\psi_2}{\partial z})^2dz\,,\hat{P}_{ij}=\int_{-h/2}^{h/2}\lambda\frac{\psi_2 z^i}{(R+z)^j}\frac{\partial\psi_2}{\partial z}dz$$

$$\square_{ij}=\int_{-h/2}^{h/2}\lambda\frac{\psi_1\psi_2 z^i}{(R+z)^j}dz\,,\square_{ij}=\int_{-h/2}^{h/2}\lambda\frac{(\psi_2)^2 z^i}{(R+z)^j}dz$$

$$\overline{H}_{ij}=\int_{-h/2}^{h/2}\lambda\frac{(\psi_1)^2 z^i}{(R+z)^j}dz\,,\square_{ij}=\int_{-h/2}^{h/2}\lambda\frac{z^i}{(R+z)^j}(\frac{\partial\psi_1}{\partial z})^2dz$$

$$\overline{P}_{ij}=\int_{-h/2}^{h/2}\lambda\frac{\psi_1 z^i}{(R+z)^j}\frac{\partial\psi_1}{\partial z}dz$$

$$a_1=-(1-\upsilon)(RF_{00}+F_{10})\,,a_2=-(\frac{1-2\upsilon}{2})F_{01}$$

$$a_3=-(\frac{1}{2})F_{00}\,,a_4=-\upsilon G_{00}-\upsilon(RQ_{00}+Q_{10})$$

$$a_5=-\upsilon F_{00}\,,a_6=(1-\upsilon)(RF_{10}+F_{20})$$

$$a_7=(1-\upsilon)F_{11}\,,a_8=-\upsilon F_{00}\,,a_9=(1-\upsilon)(RH_{00}+H_{10})$$

$$a_{10}=(1-\upsilon)H_{01})\,,a_{11}=-(RI_{00}+I_{10}),a_{12}=-(L_1)^2 a_{11}$$

$$a_{13}=(L_1)^2 I_{01}\,,a_{14}=(RI_{10}+I_{20})\,,a_{15}=-(L_1)^2 a_{14}$$

$$a_{16}=-(L_1)^2 I_{11}\,,a_{17}=(RJ_{00}+J_{10})\,,a_{18}=-(L_1)^2 a_{17}$$

$$a_{19}=-(L_1)^2 J_{01}$$

$$b_1=-(\frac{1}{2})F_{00}\,,b_2=(\frac{1-2\upsilon}{2})F_{01}$$

$$b_3=-(1-\upsilon)F_{01}\,,b_4=-(\tfrac{1-2\upsilon}{2})(RF_{00}+F10)$$

$$b_5=-(\tfrac{3-4\upsilon}{2})G_{01}-\upsilon Q_{00}\,,b_6=-(1-\upsilon)F_{01}-(1-2\upsilon)F_{12})$$

$$b_7=(1-\upsilon)F_{12}\,,b_8=(1-\upsilon)F_{10}\,,$$

$$b_9=-(1-2\upsilon)H_{02}-(1-\upsilon)F_{01}-(\tfrac{1-2\upsilon}{2})G_{01}$$

$$b_{10}=(1-\upsilon)H_{02}\,,b_{11}=(1-\upsilon)H_{00}$$

$$b_{12}=-(RI_{00}+I_{10}),b_{13}=-(L_1)^2 b_{12}$$

$$b_{14}=(L_1)^2 I_{01}\,,b_{15}=I_{10}\,,$$

$$b_{16}=-(L_1)^2 I_{10}\,,b_{17}=-(L_1)^2 I_{12}$$

$$b_{18}=J_{00}\,,b_{19}=-(L_1)^2 b_{18}$$

$$b_{20}=-(L_1)^2 J_{02}$$

$$c_1=\upsilon(RQ_{00}+Q_{10}+G_{00})\,,c_2=\upsilon Q_{00}+(\frac{3-4\upsilon}{2})G_{01}$$

$$c_3=(1-\upsilon)(R\hat{Q}_{00}+\hat{Q}_{10}+\square_{01})+2\upsilon\hat{G}_{00}\,,$$

$$c_4=-(\frac{1-2\upsilon}{2})(R\square_{00}+\square_{10})\,,c_5=-(\frac{1-2\upsilon}{2})\square_{01}\,,$$

$$c_6=(1-\upsilon)G_{01}+\upsilon Q_{00}\,,c_7=-\upsilon Q_{11}-(2-3\upsilon)G_{12}\,,$$

$$c_8=-\upsilon(RQ_{10}+Q_{20}+G_{10})\,,c_9=\upsilon Q_{00}+(1-\upsilon)G_{01}\,,$$

$$c_{10}=-\upsilon\hat{H}_{01}-(\frac{1-2\upsilon}{2})\square_{01}-(2-3\upsilon)\square_{02}$$

$$c_{11}=-\upsilon(R\hat{H}_{00}+\hat{H}_{10}+\square_{00})-(\frac{1-2\upsilon}{2})(R\square_{00}+\square_{10})$$

$$c_{12}=-(RK_{00}+K_{10})\,,c_{13}=-(L_1)^2 c_{12}\,,c_{14}=(L_1)^2 K_{01}$$

$$c_{15}=-(RL_{00}+L_{10})\,,c_{16}=-(L_1)^2 c_{15}\,,c_{17}=(L_1)^2 L_{01}$$

$$c_{18}=c_{15}\,,c_{19}=c_{16}\,,\ c_{20}=c_{17}$$

$d_1=\upsilon F_{00}, d_2=-(1-\upsilon)F_{11}$

$d_3=-(1-\upsilon)(RF_{10}+F_{20}), d_4=(1-\upsilon)F_{01}+(1-2\upsilon)F_{12}$

$d_5=-(1-\upsilon)F_{12}, d_6=-(1-\upsilon)F_{10}$

$d_7=(1-\upsilon)G_{01}+\upsilon Q_{00}, d_8=-\upsilon Q_{11}-(2-3\upsilon)G_{12}$

$d_9=-\upsilon G_{10}-\upsilon(RQ_{10}+Q_{20}), d_{10}=(1-\upsilon)F_{01}+K_w$

$d_{11}=-2\upsilon F_{10}-(L_1)^2K_w-G$

$d_{12}=-2(1-\upsilon)F_{12}-2(1-2\upsilon)F_{23}-\dfrac{(L_1)^2K_w+G}{(R+h/2)^2}$

$d_{13}=(1-2\upsilon)F_{23}+\dfrac{(L_1)^2G}{(R+h/2)^4}, d_{14}=2(1-\upsilon)F_{21}+\dfrac{2(L_1)^2G}{(R+h/2)^2}$

$d_{15}=(1-\upsilon)(RF_{20}+F_{30})+(L_1)^2G, d_{16}=(1-\upsilon)F_{01}+K_w$

$d_{17}=-\upsilon(H_{00}+F_{10})-G-(L_1)^2K_w$

$d_{18}=-(1-\upsilon)(F_{12}+H_{02})-(1-2\upsilon)(G_{12}+2H_{13})-\dfrac{(L_1)^2K_w+G}{(R+h/2)^2}$

$, d_{19}=(1-\upsilon)H_{13}+\dfrac{(L_1)^2G}{(R+h/2)^4}, d_{20}=2(1-\upsilon)H_{11}+\dfrac{2(L_1)^2G}{(R+h/2)^2}$

$d_{21}=(1-\upsilon)(RH_{10}+H_{20})+(L_1)^2G$

$d_{22}=-(RI_{10}+I_{20}), d_{23}=-(L_1)^2d_{22}$

$d_{24}=(L_1)^2I_{11}, d_{25}=-I_{10}, d_{26}=-(L_1)^2d_{25}$

$d_{27}=(L_1)^2I_{12}, d_{28}=-(RL_{00}+L_{10})$

$d_{29}=-(L_1)^2d_{28}, d_{30}=(L_1)^2L_{01}$

$d_{31}=-(RI_{00}+I_{10}), d_{32}=(RI_{20}+I_{30})-(L_1)^2d_{31}$

$d_{33}=I_{21}+(L_1)^2I_{01}, d_{34}=-(L_1)^2(RI_{20}+I_{30})$

$d_{35}=-2(L_1)^2I_{21}, d_{36}=-(L_1)^2I_{23}, d_{37}=-(RI_{00}+I_{10})$

$d_{38}=(RJ_{10}+J_{20})-(L_1)^2d_{37}, d_{39}=J_{11}+(L_1)^2I_{01}$

$d_{40}=-(L_1)^2(RJ_{10}+J_{20}), d_{41}=-2(L_1)^2J_{11}$

$d_{42}=-(L_1)^2J_{13}$

$e_1=\upsilon F_{00}, e_2=-(1-\upsilon)H_{01}, e_3=-(1-\upsilon)(RH_{00}+H_{10})$

$e_4=(1-\upsilon)F_{01}+(1-2\upsilon)H_{02}+\dfrac{1-2\upsilon}{2}G_{01}$

$e_5=-(1-\upsilon)H_{00}, e_6=-(1-\upsilon)H_{02}$

$e_7=(1-\upsilon)G_{01}+\upsilon Q_{00}, e_8=-(2-3\upsilon)\overset{\square}{H}_{02}-\upsilon\hat{H}_{01}-\dfrac{1-2\upsilon}{2}\overset{\square}{G}_{01}$

$e_9=-\upsilon(\overset{\square}{H}_{00}+R\hat{H}_{00}+\hat{H}_{01})-\dfrac{1-2\upsilon}{2}(R\overset{\square}{G}_{00}+\overset{\square}{G}_{10})$

$e_{10}=(1-\upsilon)F_{01}+K_w, e_{11}=-\upsilon(F_{10}+H_{00})-(L_1)^2K_w-G$

$e_{12}=-(1-\upsilon)(H_{02}+F_{12})-(1-2\upsilon)(2H_{13}+G_{12})-\dfrac{(L_1)^2K_w+G}{(R+h/2)^2}$

$e_{13}=(1-\upsilon)H_{13}+\dfrac{(L_1)^2G}{(R+h/2)^4}, e_{14}=2(1-\upsilon)H_{11}+\dfrac{2(L_1)^2G}{(R+h/2)^2}$

$e_{15}=(1-\upsilon)(RH_{10}+H_{20})+(L_1)^2G, e_{16}=(1-\upsilon)F_{01}+K_w$

$e_{17}=-2\upsilon H_{00}-\dfrac{1-2\upsilon}{2}(R\overset{\square}{G}_{00}+\overset{\square}{G}_{10})-G-(L_1)^2K_w$

$e_{18}=-2(1-\upsilon)H_{02}-\dfrac{1-2\upsilon}{2}(\overset{\square}{G}_{01}+4\overset{\square}{H}_{02}+4\overline{H}_{03})-\dfrac{(L_1)^2K_w+G}{(R+h/2)^2}$

$e_{19}=(1-\upsilon)\overline{H}_{03}+\dfrac{(L_1)^2G}{(R+h/2)^4}, e_{20}=2(1-\upsilon)\overline{H}_{01}+\dfrac{2(L_1)^2G}{(R+h/2)^2}$

$e_{21}=(1-\upsilon)(R\overline{H}_{00}+\overline{H}_{10})+(L_1)^2G$